Journal of Catalysis 292 (2012) 53–63

Contents lists available at SciVerse ScienceDirect

Journal of Catalysis

journal homepage: www.elsevier.com/locate/jcat

Investigation of the selective catalytic reduction of nitric oxide with ammonia over Mn/TiO_2 catalysts through transient isotopic labeling and *in situ* FT-IR studies

Padmanabha Reddy Ettireddy, Neeraja Ettireddy, Thirupathi Boningari, Robert Pardemann, Panagiotis G. Smirniotis *

Chemical Engineering Program, School of Energy, Environmental, Biological and Medicinal Engineering, University of Cincinnati, Cincinnati, OH 45221-0012, USA

ARTICLE INFO

Article history:
Received 27 January 2012
Revised 20 April 2012
Accepted 23 April 2012
Available online 14 June 2012

Keywords:
Isotopic labeling
In situ FT-IR
Low-temperature SCR
Ammonia oxidation
^{15}NO
$^{15}NH_3$
$^{18}O_2$

ABSTRACT

The transient isotopic labeling studies were performed under steady state conditions by using ^{15}N (^{15}NO and $^{15}NH_3$) and ^{18}O ($^{18}O_2$) containing species to investigate the reaction mechanism of the low-temperature SCR of NO over Mn/TiO_2. Our investigation has suggested that the nitric oxide forms neither nitrous oxide nor it is oxidized to nitrogen dioxide with the gas phase oxygen. The results acquired with the time resolution illustrated that the reaction of ammonia with lattice oxygen was practically instantaneous. The formation of labeled $N_2{}^{18}O$, $N^{18}O$, and $H_2{}^{18}O$ species is evident through the NH_3 contact with catalyst surface lattice oxygen but not direct contact with the gas phase oxygen. This is consistent with the view that the lattice oxygen of Mn/TiO_2 catalyst has direct effect on the reaction mechanism rather than gas phase oxygen. Our labeling experiments suggest that the SCR reaction rate is very small in the absence of gas phase oxygen and enhanced distinctly by the addition of excess oxygen. The cross-labeled $^{15}N^{14}N$ is the dominant form of nitrogen during the NH_3 labeling studies. The increase in the SCR reaction temperature monotonically enhanced the ammonia oxidation. The evolution of $^{15}N^{14}N$, $^{15}N^{14}NO$, and ^{15}NO species from the labeled ammonia ($^{15}NH_3$) and unlabeled nitric oxide (^{14}NO) revealed the occurrence of ammonia oxidation. The results obtained in these experiments were combined with oxygen exchange experiments to arrive at conclusions regarding the plausible mechanism of the SCR reaction. The oxygen exchange between nitric oxide and the catalyst lattice oxygen established in the catalytic reduction of NO reaction. The effect of oxygen on activity and selectivity is noteworthy in both SCR and ammonia oxidation reactions over Mn/TiO_2. The role of ammonia oxidation has been quantified for the overall SCR reaction network at low-temperatures. The role of ammonia oxidation and surface oxygen species has been addressed to substantiate the conclusions drawn.

1. Introduction

In recent years, manganese-based catalysts have attracted much attention because their unique redox (oxidation–reduction cycle) properties make them useful for a variety of applications [1–4]. Moreover, Mn-based catalysts have proven to be the most active catalysts for the low-temperature selective catalytic reduction (SCR) of NO_x [5–9]. In spite of the rapidly growing commercial applications for the SCR process and the large number of researchers focusing on various aspects of these reactions, there still remain questions about the reaction pathway and the potential intermediate species over these catalysts. A clear picture of the reaction mechanism can be obtained by investigating the interactions between different isotopic labeled species, using transient response analysis and *in situ* FT-IR. In this way, information is obtained on the elementary steps of a reaction, since the time-resolved observations allow quantitative assessment of the accumulation of species on the surface [10,11]. A few isotopic labeling studies over the Fe-zeolites (NH_3-SCR) [12], V_2O_5 (NH_3-SCR) [13,14], Ag/Al_2O_3 (HC-SCR) [15], Cr_2O_3 (NH_3-SCR) [16], $La_{0.8}Ce_{0.2}MnO_3$ (CO oxidation) [17], MoO_3 (CH_4 oxidation) [18] have recently been reported, but to date no transient isotopic labeling studies with *in situ* FT-IR have been reported to investigate the reaction mechanism over Mn/TiO_2 catalysts.

Our group developed an inexpensive manganese-based catalysts, which manifested high activity and nitrogen selectivity even in the presence of 10 vol.% water for low-temperature SCR [5–9,19]. We have also demonstrated the structural sensitivity of low-temperature NO reduction in the presence NH_3 over TiO_2 (Hombikat) supported manganese oxide catalysts. It was realized that the oxidation of ammonia is an important step to determine the selectivity of low-temperature SCR reaction. In our recent paper, we presented *in situ* FT-IR data to propose a tentative reaction mechanism for the low-temperature SCR of NO with NH_3 [20]. We have found that a combination of moderately strong monodentate and bidentate nitrate species, along with a split in the symmetric

---

* Corresponding author. Fax: +1 513 556 3473.
E-mail address: Panagiotis.Smirniotis@uc.edu (P.G. Smirniotis).

0021-9517/$ - see front matter Published by Elsevier Inc.
http://dx.doi.org/10.1016/j.jcat.2012.04.019

deformation of NH_3 coordination to Lewis acid sites, appears to be important for high activity and selectivity. It was also proposed that the reaction mechanism proceeds through the formation of nitrosamide and azoxy species [20]. In order to improve our understanding on the mechanism, additional studies involving isotopic labeled gases were performed. Our main focus is to study the involvement of surface oxygen species and its role played toward the mechanism.

In the present work, we investigated the mechanism of the selective catalytic reduction of nitric oxide with ammonia using transient labeling studies with ^{15}NO, $^{15}NH_3$, and $^{18}O_2$ over the 16.7% Mn/TiO_2 (Hombikat) catalyst. This catalyst demonstrated high activity and selectivity in our previous studies [9]. The reaction pathways have been examined by switching selected combination of gases, both labeled and unlabeled (NO, NH_3, and O_2). The underlying thought was to investigate the role of surface labile oxygen and thus propose the mechanism for the low-temperature reduction of NO with NH_3 reaction. By using the transient studies of labeled gases, we have found that the surface oxygen species play an important role in the low-temperature SCR reaction. However, the results acquired with the time resolution illustrated that the reaction of ammonia with lattice oxygen was practically instantaneous. The formation of N_2O, NO, and H_2O species is evident when ammonia came into contact with catalyst lattice oxygen. It is remarkable to note that the formation of NO_2 was not observed over the Mn/TiO_2 catalyst. The formation of cross-labeled species during the transient studies revealed the occurrence of ammonia oxidation. In connection with the transient isotopic labeling and *in situ* FT-IR studies, plausible mechanism for the low-temperature SCR of NO_x over titania-supported manganese catalysts is proposed and the reaction is more likely a Mars–van-Krevelen type mechanism.

2. Experimental

2.1. Catalysts preparation

The TiO_2 used in this study was Hombikat UV 100 from Sachtleben Chemie. As determined by N_2 adsorption, it had a specific surface area of 309 m^2/g, a pore volume of 0.37 cm^3/g, and a pore diameter of 4.5 nm. In a typical synthesis, 50 mL of deionized water was added to a 100 mL beaker containing 1.0 g of support. The mixture was heated to 70 °C under continuous stirring conditions. A predetermined quantity of nitrate precursor was then added, and the mixture was evaporated to dryness. The resulting material obtained was further dried overnight at 110 °C, ground, and sieved (80–120 mesh). Finally, the catalyst was calcined at 240 °C for 4 h in continuous air flow.

2.2. Characterization of catalyst

The specific surface areas were measured by nitrogen adsorption at −196 °C by the BET method using a Micromeritics Gemini 2360 surface area instrument. Prior to the analysis, 0.05–0.10 g of catalysts was degassed at 150 °C for 2 h under helium atmosphere.

XRD studies were performed on a Siemens D500 Diffractometer with a monochromated Cu Kα radiation source (wavelength 1.5406 Å). The scans were performed for 2θ values ranging from 5° to 70° with step size 0.1° and time step 1.0 s to assess the crystallinity of the manganese loading. XRD phases present in the catalyst samples were identified using JCPDS powder data files.

X-ray photoelectron spectroscopy (XPS) was used to analyze the atomic surface concentration on each catalyst. The spectra were recorded on a Perkin–Elmer Model 5300 X-ray photoelectron spectrometer using Mg Kα (1253.6 eV) as a radiation source at 300 W. The spectra were recorded in the fixed analyzer transmission mode with pass energies of 89.45 and 35.75 eV for recording survey and high-resolution spectra, respectively. The powdered catalysts were mounted onto the sample holder and degassed overnight at room temperature at a pressure on the order of 10^{-7} torrs. Sample charging effects were eliminated by correcting the observed spectra with the C 1*s* binding energy (BE) value of 284.6 eV. An estimated error of 0.1 eV can be considered for all the measurements.

Oxygen pulse chemisorption measurements were performed to determine the dispersion of manganese on the support surface. Helium was used as the carrier gas (30 mL/min). Before analysis, approximately 50 mg of catalyst samples was reduced in flowing 10% H_2 in helium (50 mL/min) at 250 °C for 2 h and then flushed for 30 min in prepurified helium at the same temperature. Then, oxygen pulses (1 mL loop volume) were injected onto the carrier gas until saturation of the sample was attained. The oxygen uptake was quantified by a TCD connected to a Micromeretics Autochem 2910 instrument.

In situ FT-IR spectra were recorded using a Bio-Rad (FTS-40) Fourier transform instrument and a heatable IR cell connected to a conventional volumetric operator. The scans were collected at a scan speed of 5 kHz, resolution of 2.0, and an aperture opening of 2.0 cm^{-1}. Sixteen scans were averaged for each normalized spectrum. Circular self-supporting thin wafers (8 mm diameter) consisting of 12 mg of material were used for the study. The wafers were placed in a high-temperature cell with CaF_2 windows and purged *in situ* in the IR cell with prepurified grade helium (30 mL min^{-1}, Wright Brothers) at 473 K for 2 h to remove any adsorbed impurities. Then, the samples were cooled to 323 K, and the selected gasses were introduced into the cell with a flow of 30 mL min^{-1} for 1 h at 323 K to ensure complete saturation of the sample. Physisorbed gasses were removed by flushing the wafer with prepurified helium for 3 h at 373 K. Subsequently, the *in situ* FT-IR spectra were recorded by evacuation at different temperatures.

2.3. Reaction studies

The premixed gases namely oxygen (4% in He, Wright Brothers), ammonia (3.99% in He, Wright Brothers), and nitric oxide (2.0% in He, Matheson) were used as received. The labeled gases were isotopic oxygen (4% $^{18}O_2$ (99 atom%) in balance helium, Isotech), ammonia (4.06% $^{15}NH_3$ (98 atom%) in balance helium, Isotech), and nitric oxide (2.54% ^{15}NO (99 atom%) in balance helium, Icon). The labeled SCR reaction experiments were performed using a feed mixture of 2500 ppm nitric oxide, 2500 ppm ammonia, and 2 vol.% oxygen with helium as the balance gas (reaction 1).

$$4NO + 4NH_3 + O_2 \rightarrow 4N_2 + 6H_2O$$

A 50–70 mg of catalyst sample was used in this experiment. The reactions were performed at 175 °C and total flow rate was 50 mL/min. The catalyst was first pretreated at reaction temperature for two hours with oxygen. After the pretreatment, the reactions were carried out at the steady state for two hours with unlabeled components before switched to labeled gas. The experiments for the investigation of the interaction of the catalyst oxygen with the gas phase oxygen and the nitric oxide were done by using 150 mg of catalyst.

A MKS PPT Quadrupole Residual Gas Analyzer was used to detect the species at their different atomic mass units (amu). The signals of ammonia needed to be corrected from the interference with oxygen by using the relative intensities of the $m/e = 32$ and $m/e = 16$ peak. The data for the correction are obtained from calibration experiments. The water peak at $m/e = 18$ was corrected from the interference with ammonia and oxygen. From the nitric oxide peaks, the influence of the oxygen was subtracted. For none of the nitrous oxide species, a correction was necessary. To get the normalized concentrations for each species, the partial pressure of the species was divided by the sum of the partial pressures of all species of the same type.

3. Results and discussion

3.1. Characterization of the catalyst sample

The physico-chemical characteristics of the investigated catalyst system are presented in Table 1. The BET surface area of the commercial TiO_2 anatase (Hombikat) sample used in the preparation of the catalyst was found to be 309 $m^2\,g^{-1}$ whereas that of Mn loaded TiO_2 catalyst calcined at 240 °C was found to be 196 $m^2\,g^{-1}$. This is as expected due to the blocking of the micropores of the titania surface after calcination. In general, the surface area of the final catalyst material decreases with increasing quantity of the active component until the monolayer coverage of the impregnated component is completed [21].

The X-ray powder diffraction pattern of MnO_x/TiO_2 contains very sharp peaks which correspond to anatase phase (JCPDS #71-1169). The pattern also shows X-ray reflections which are attributed to the formation of crystalline manganese oxide (MnO_2) phase. The X-ray reflections at d = 2.41, 1.63, and 2.11 Å (MnO_2 phase (JCPDS #04-0779)) can be observed [20]. Conversely, the binding energy values for different XPS peaks (O1*s*, Ti2*p*, and Mn 2*p*) are shown in Table 1, which agrees well with that reported in the literature. As presented in the table, the binding energy value of Mn $2p_{3/2}$ for the catalyst is 642 eV, probably corresponding to the Mn^{4+} state [6,22]. It is known that at lower loading, the XPS peak of Mn 2*p* appeared to be very broad with very small shoulders. This is due to the presence of different oxidation states of Mn along with major Mn^{4+} species, and the shoulder peak disappears at higher loadings [9]. The pattern thus shows the presence of MnO_2 as the major phase. The sharp intensity of the Mn $2p_{3/2}$ peak hints the strong interaction of Mn with TiO_2 anatase support. Due to this interaction, the catalyst is expected to render high activity and selectivity toward low-temperature SCR of NO with NH_3 as the reductant.

The Mn2*p*/Ti2*p* ratio was calculated to measure the relative dispersion of manganese oxide on the support surface. The surface atomic ratio of Mn/Ti is found to be 0.28 that is relatively large, thus indicating that the support surface is covered by manganese oxide. It leads to the completion of monolayer coverage, and therefore, the manganese oxide is present in polymeric or microcrystalline form.

The dispersion, defined as the percent of Mn-oxide units available for reduction and subsequent oxygen uptake, is estimated from the total number of Mn-oxide units present in the sample and the number of oxygen atoms chemisorbed. As presented in Table 1, the oxygen chemisorption capacity and the metal dispersion (%) of the catalyst are significantly high which may eventually lead to better catalytic activity.

3.2. Isotopic labeling and in situ FT-IR studies

The main intention of the labeled studies was to improve our understanding on the catalytic surface mechanism by involving surface oxygen species. The reaction mechanism for the SCR of NO_x on MnO_x/TiO_2 catalysts with NH_3 as reductant was proposed by Pena et al. [20], which is based on the results obtained from *in situ* FT-IR studies. To better understand the mechanism and the role of the lattice oxygen from the catalyst surface, it is necessary to elucidate since no such observation was made based on the results from the FT-IR studies. In the present study, the first set of experiments was performed with individual gases to better understand the role and the interaction of the reactants. Initially, the interaction of the catalyst with the gas phase oxygen was investigated followed by the study of the behavior of NO species. The goal of these experiments was to find (i) the strength and the role of the labile oxygen atom on the catalyst surface, (ii) the limitation in the direction of potential labile oxygen exchange with labeled oxygen, and (iii) whether there is any interaction of the nitric oxide oxygen with the catalyst surface. The second set of experiments was considered to determine the origin of ammonia oxidation and SCR products. For this purpose, the ammonia oxidation was assayed with labeled oxygen and the regular SCR reaction was carried out with isotopic ammonia, isotopic oxygen, and isotopic nitric oxide. Conclusions about surface residence times of certain gases could be drawn from the shape of the transient curves of certain species, since the evolution of the transient curves of all important species could be observed with the mass spectrometer.

3.2.1. Interaction between the oxygen from catalyst surface and the gas phase oxygen ($^{16}O_2$ switched to $^{18}O_2$)

In this experiment, the catalyst was pretreated at reaction temperature (175 °C) in the normal way with unlabeled oxygen ($^{16}O_2$). The purpose of the pretreatment was to remove the OH-groups from the catalyst surface. Following this, the system was flushed with helium to completely remove any residual gas containing unlabeled oxygen from the reactor. After this step, labeled oxygen ($^{18}O_2$) was introduced to the system and the amu for $^{16}O_2$ (m/e = 32), $^{16}O^{18}O$ (m/e = 34), and $^{18}O_2$ (m/e = 36) were observed with the mass spectrometer (Fig. 1). The signal of the cross-labeled oxygen ($^{16}O^{18}O$) was corrected from the interference with the labeled oxygen.

As can be seen from Fig. 1, when labeled oxygen was fed through the catalyst bed, an increase of the cross-labeled oxygen was observed. This indicates that some oxygen exchange takes place with the lattice oxygen from the catalyst (Eq. (1)).

$$Mn^{16}O_x + {}^{18}O_2 \rightarrow Mn^{18}O_x + {}^{16}O_2 \qquad (1)$$

Evidently, the ^{16}O atom must be due to unlabeled lattice oxygen, while the ^{18}O atom comes from the gas phase oxygen. The formation of the cross-labeled oxygen from unlabeled gas phase oxygen in the system should be ruled out. After the catalyst pretreatment with $^{16}O_2$, the catalyst bed was flushed with helium for one hour at reaction temperature, and no increase of the signal for unlabeled oxygen ($^{16}O_2$) was observed during the active experiment. However, the total amount of cross-labeled oxygen was small in comparison with the total amount of gas. Only 1.4% of

Table 1
Physico-chemical characteristics of 16.6 wt.% Mn/TiO_2 catalyst.

BET SA (m^2/g)	O_2 uptake (μmol/g cat)	Dispersion	Site density[a] ($10^{17}/m^2$)	STY[b] at 100,000 GHSV	Binding energy (eV)					
					Ti $2p_{3/2}$	Ti $2p_{1/2}$	O 1*s*	Mn $2p_{3/2}$	Mn $2p_{3/2}$	Mn/Ti
196	882	0.58	27.10	127.8	458.5	464.2	529.7	642.0	653.7	0.28

[a] Oxygen atom site density: number of oxygen atom chemisorbed per m^2 of surface, coordinatively unsaturated oxygen vacancies/sites (CUS).
[b] Site time yield (STY): number of NO molecules converted per manganese atom site per second.

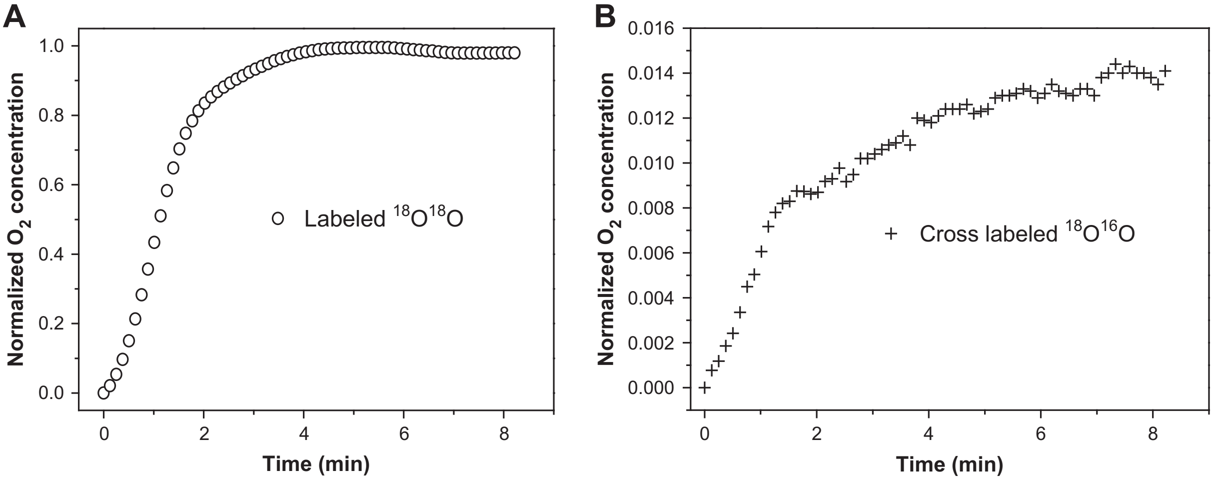

Fig. 1. (A) normalized oxygen ($^{18}O_2$) concentration, and (B) normalized cross-labeled oxygen ($^{16}O^{18}O$) concentration depending as a function of time in the experiment which investigated the interaction of gas phase labeled oxygen.

the gas phase oxygen interacted with the catalyst (0.15 g). Since the gas phase concentration of the oxygen was 20,000 ppm, the cross-labeled oxygen was about 280 ppm after nine minutes. This implies that although the lattice oxygen is capable of interacting with the oxygen from the gas phase, the lability of the bulk catalyst oxygen on the surface is relatively small, especially when the amount of used catalyst is concerned.

3.2.2. Interaction between nitric oxide and the catalyst surface

This study was performed to analyze the oxygen exchange between nitric oxide and the catalyst. In this case, the unlabeled oxygen on the catalyst surface was replaced by labeled oxygen ($^{18}O_2$). To replace the unlabeled oxygen, the catalyst was reduced after the pretreatment by exposing ammonia to the catalyst without addition of oxygen. Consequently, ammonia reduced the surface oxygen ion leading to the oxygen vacancies over the catalyst as a result of the ammonia oxidation reaction. After the ammonia oxidation, the system was flushed with helium and the catalyst was exposed to labeled oxygen ($^{18}O_2$), which replaced the missing surface oxygen. The system was flushed with helium again before nitric oxide ($N^{16}O$) was led to the reactor. To detect potential oxygen exchange, the amu for $N^{16}O$ (30) and $N^{18}O$ (32) were recorded. It was found that oxygen exchange between nitric oxide and the catalyst oxygen takes place (Fig. 2). When the nitric oxide was introduced, not only the peak for $N^{16}O$ but also the signal for $N^{18}O$ has significantly increased. However, the total amount of the labeled species was less in comparison with the amount of unlabeled nitric oxide and the $N^{18}O$ signal developed with a short delay in time in comparison with the $N^{16}O$. This result implies that the $N^{18}O$ arose from nitric oxide ($N^{16}O$), which adsorbed on the catalyst surface and exchanged its own oxygen with labeled oxygen from the catalyst surface. Although it was reported that no nitric oxide can adsorb at temperatures higher than 50 °C, the result of *in situ* FT-IR studies showed that nitric oxide adsorbs on the catalyst also at 175 °C (reaction temperature) [23]. The signal of the labeled $N^{18}O$ decreased relatively fast after reaching a maximum (not shown), because on sites are capable of adsorbing nitric oxide. The labeled oxygen on the surface must have been replaced by unlabeled oxygen from the nitric oxide (Eq. (2)).

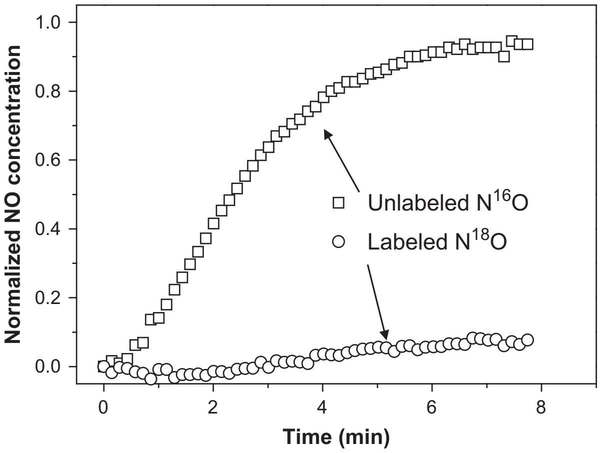

Fig. 2. Normalized nitric oxide concentrations as a function of time in the experiment for the investigation of the nitric oxide interaction with the labeled lattice ^{18}O.

$$Mn^{18}O_x + N^{16}O \rightarrow N^{18}O + Mn^{16}O_x \quad (2)$$

3.2.3. Investigation of the reaction of NO + O_2 (NO + $^{16}O_2$ switched to NO + $^{18}O_2$)

In order to investigate if the nitric oxide performs any reaction with oxygen on the catalyst, the oxygen was labeled to $^{18}O_2$ after the unlabeled gas was passed through the reactor for two hours. The mass numbers of the potential products namely $N^{16}O$ ($m/e = 30$), $N_2{}^{16}O$ ($m/e = 44$), $N_2{}^{18}O$ ($m/e = 46$), $N^{16}O_2$ ($m/e = 46$), $N^{16}O^{18}O$ ($m/e = 48$), and $N^{18}O_2$ ($m/e = 50$) were considered. The collected data at the steady state of the reaction before and the pseudosteady state after the labeled species were admitted, suggested that there was no increase in the intensity of any peak. Therefore, it can be concluded that when the catalyst is exposed to nitric oxide and oxygen, the nitric oxide does not form either nitrous oxide or it is oxidized to form nitrogen dioxide (Eq. (3)).

$$Mn^{18}O_x + N^{16}O + {}^{16}O_2 \rightarrow N^{18}O + {}^{18}O_2 + Mn^{18}O_{x-3}{}^{16}O_3 \quad (3)$$

3.2.4. An in situ FT-IR investigation (NO adsorbed and NO + O_2 co-adsorbed)

To support the above statement and to gain insight for the interaction of NO with the gas phase oxygen, the adsorption and desorption characteristics of NO and NO + O_2 over the Mn/TiO$_2$ catalyst have been investigated. The *in situ* FT-IR spectra of NO adsorbed and NO + O_2 co-adsorbed over the Mn/TiO$_2$ catalyst followed by evacuation at 175 °C and 300 °C temperatures are presented in Fig. 3. *In situ* contact of NO led to the formation of a number of peaks that can be basically attributed to the formation of two types of nitrates on the surface of the material tested, namely monodentate and bidentate nitrates. The absorption peaks at 1242, 1295, and 1498 cm^{-1} could be assigned to monodentate nitrate species, while the remaining peaks at 1583 and 1610 cm^{-1} are ascribed to bidentate nitrate species [24]. The weak absorption peak at 1526 cm^{-1} has been interpreted as the split v_3 mode of bidentate nitrates [25,26]. The desorption of NO or $NO + O_2$ over Mn/TiO_2 at 300 °C led to the formation of new absorption peaks at 1285 and 1338 cm^{-1} which are attributed to the N_2O_{ads} species over the surface of catalyst. During the present study, the absorption band at 1632 cm^{-1} region was not observed which corresponds to the asymmetric stretching of coordinatively held NO_2 (1617 cm^{-1} in the gas phase) [27,28]. The absence of absorption bands in the region of 1423–1470 cm^{-1} and 1957–2033 cm^{-1} correspond to the asymmetric vibrations of NO_2 (v_{as}-NO_2) and assignments of $ON—Mn^{n+}—ONO_2^-$, respectively. These results suggest that the nitric oxide does not get oxidized to NO_2 over the surface of Mn/TiO_2 even in the presence of excess oxygen [25].

These results are in agreement with our transient labeling studies, where the nitric oxide does not form N_2O or NO_2 with the gas phase oxygen at 175 °C. This is a clear evidence that neither the peak positions nor the intensity of the peaks changed significantly in the presence of gas phase oxygen ($NO + O_2$). Therefore, the nitrate species observed in the FT-IR spectra suggest that the lattice oxygen from the surface of the catalyst rather than gas phase oxygen plays a significant role in the formation of nitrates (Eqs. (4), (5)).

$$Mn^{n+} + NO \rightarrow Mn^{n+} - NO \quad (4)$$

$$MnO_x + 2NO + 2O_2 \rightarrow {}_xOMn - O_2 - NO + {}_xOMn - O - NO_2 \quad (5)$$

In situ experiments bring in contact nitrous oxide with Mn/TiO_2 catalyst followed by degassing at 175 °C and 300 °C temperatures cause the formation of absorption bands at 1161, 1251, 1285, 1338, and 1576 cm^{-1} (Fig. 4). The appearance of the new peaks at 1285 and 1338 cm^{-1} was observed in the case of NO adsorption and $NO + O_2$ co-adsorption when the temperature was raised up to 300 °C (Fig. 3). From both figures (Figs. 3 and 4), it is clear that N_2O_{ads} is formed during the high-temperature reaction at 300 °C. Our *in situ*–FT-IR studies suggest that the nitric oxide does not form either nitrous oxide or nitrogen dioxide over the surface of Mn/TiO_2 at low-temperatures. Labile oxygen from the surface of the catalyst plays an important role rather than excess gas phase oxygen.

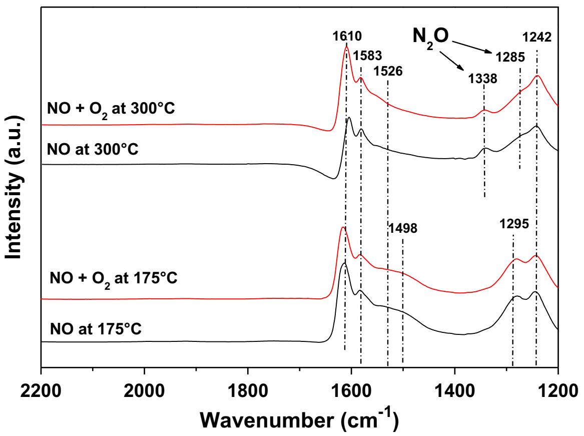

Fig. 3. *In situ* FT-IR spectra of NO adsorption and $NO + O_2$ co-adsorption over the Mn/TiO_2 catalyst, degassing at 175 °C and 300 °C.

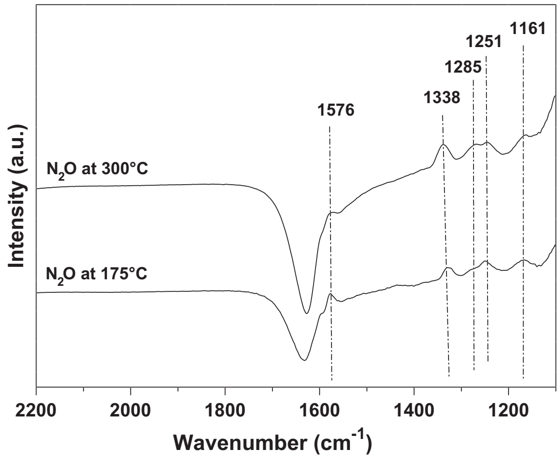

Fig. 4. *In situ* FT-IR spectra of N_2O adsorption over the Mn/TiO_2 catalyst.

3.2.5. Investigation of the ammonia oxidation reaction ($NH_3 + {}^{16}O_2$ switched to $NH_3 + {}^{18}O_2$)

The ammonia oxidation reaction was investigated independently under typical reaction conditions prior to the SCR reaction. For this purpose, the catalyst was exposed to ammonia and oxygen. When the reaction was at the steady state, the oxygen was switched from ${}^{16}O_2$ to ${}^{18}O_2$. The goal of this experiment was to find out (i) the oxidation products if any, (ii) the amount of oxidation products, and (iii) the contribution of oxygen of different origin (lattice oxygen from the catalyst surface or gas phase oxygen) to the different oxidation products. Products arising from ammonia oxidation are nitrogen, nitric oxide, nitrous oxide, and water [13,14,29]. The transient curves for oxygen, water species, and nitrous oxide are presented in Fig. 5.

According to the *in situ* FT-IR studies, which were performed earlier, this type of catalysts showed high activity in the oxidation of ammonia [30]. The main nitrogen containing oxidation products were nitrogen (N_2) and nitric oxide while nitrous oxide was formed in relatively small amounts. As one can observe from Fig. 5, the occurrence of labeled species begins immediately after labeling the oxygen (Eqs. (6) and (7)).

$$Mn^{18}O_x + 2NH_3 + 2{}^{16}O_2 \rightarrow N_2{}^{18}O + 3H_2{}^{18}O + Mn^{18}O_{x-4}{}^{16}O_4 \quad (6)$$

$$Mn^{18}O_x + 4NH_3 + 5{}^{16}O_2 \rightarrow 4N^{18}O + 6H_2{}^{18}O + Mn^{18}O_{x-10}{}^{16}O_{10} \quad (7)$$

The formation of labeled species $H_2{}^{18}O$, ${}^{18}O{}^{18}O$, $N_2{}^{18}O$, $N^{18}O$, and the decrease of the concentration of $H_2{}^{16}O$, $N_2{}^{16}O$, $N^{16}O$ species is indicative for the ammonia interaction with the labile oxygen. Furthermore, the sharp decrease of the unlabeled species ${}^{16}O{}^{16}O$ response (Fig. 5B open tetra angle) on NH_3 introduction (at t = fraction of minute in Fig. 5B) is evident of the instantaneous reaction of surface oxygen species with ammonia [31]. However, the fraction of the labeled species varies for each product. Nitrous oxide shows the highest fraction of labeled species after 25 min of operation of this experiment. It is interesting to note that no transient curve for any species reached a pseudosteady state even after 25 min. This indicates that the partial pressure of any product does not follow the increase of oxygen concentration in the feed. It is evident that all products are formed with lattice oxygen from the catalyst surface/subsurface and not directly with the gas phase oxygen. The labeled species arose from the reaction of ammonia with labeled oxygen which was incorporated into the catalyst lattice to fill the oxygen vacancies over the catalyst surface.

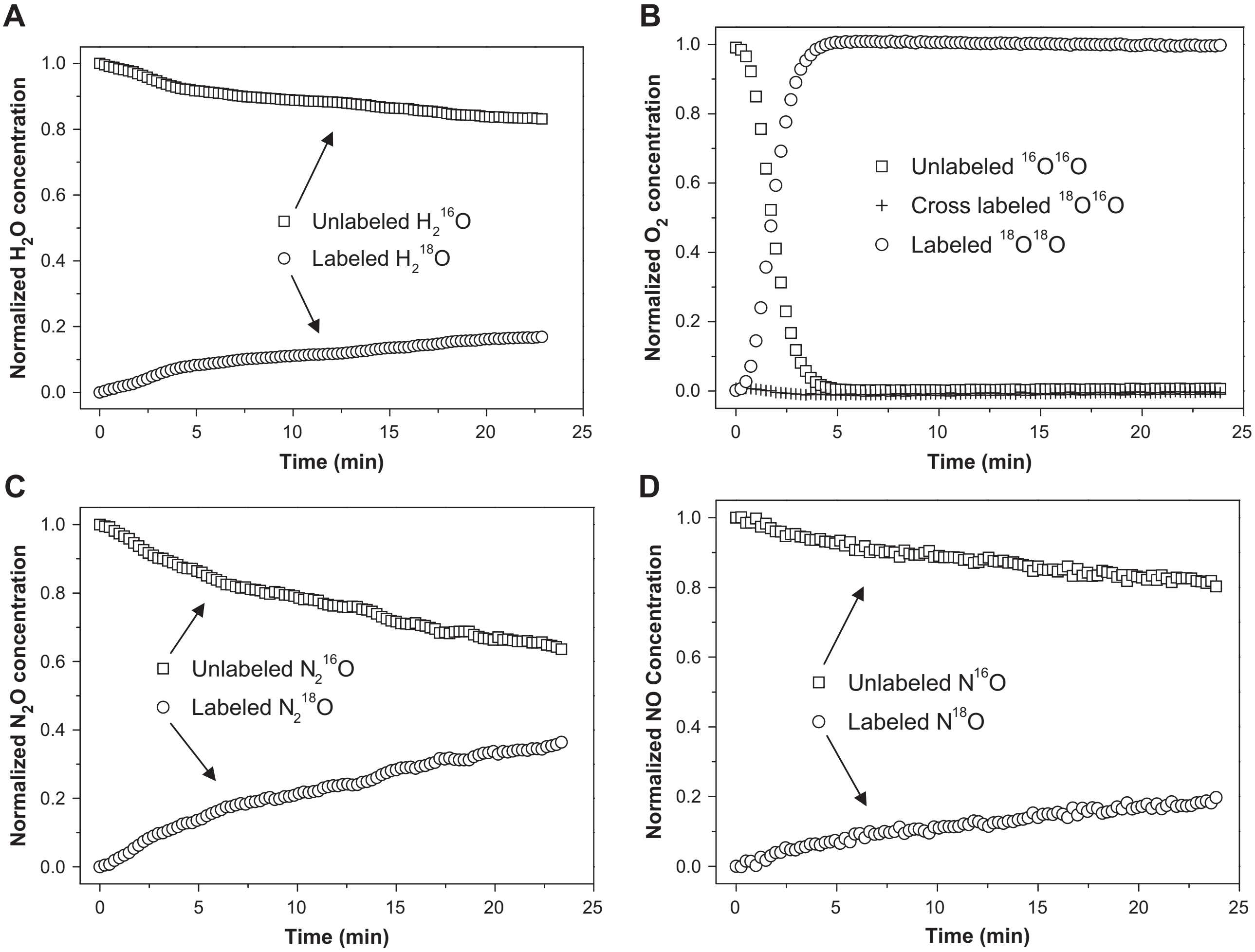

Fig. 5. Normalized concentrations of (A) water, (B) oxygen, (C) nitrous oxide, and (D) nitric oxide depending on the time in the ammonia oxidation experiment with labeled oxygen gas.

3.2.6. In situ contact of ammonia (FT-IR studies)

In situ FT-IR experiments were conducted over the titania-supported manganese catalyst to identify the reaction intermediates and to propose a plausible reaction mechanism. Ammonia adsorbed FT-IR experiments were performed at 175 and 400 °C to gain a better understanding of molecular behavior of ammonia and to acquire the information about the ammonia oxidation over the surface of Mn/TiO_2 (Fig. 6). *In situ* experiments involving the contact of ammonia with Mn/TiO_2 catalyst at 323 K and followed by degassing at 175 and 400 °C temperatures cause the formation of absorption bands at 1167, 1220, 1285, 1338, 1526, and 1610 cm^{-1}. The strong absorption peak at 1167 cm^{-1} is attributed to the δs (NH_3) bound to Lewis acid sites, which was suggested to play an important role in the low-temperature SCR [6,7,9]. Interestingly, this peak at 1167 cm^{-1} (δs NH_3 coordinated to Lewis acid sites) decreases and finally disappears after evacuation at 400 °C. The band at 1220 cm^{-1} has been assigned to the N–N stretching and NH_2 rockings [29]. Intensity of the peaks at 1285 cm^{-1} and 1338 cm^{-1} was very low at 175 °C and increased at 400 °C. These features suggest that ammonia is decomposed by heating before desorption and indicate that the oxidation of ammonia can occur over the surface of Mn/TiO_2 catalyst. The weak absorption peak at 1526 cm^{-1} is being possibly associated to split ν_3 mode of bidentate nitrates [25,26]. This is probably due to the formation of NO species by the ammonia oxidation with surface oxygen. The band at 1610 cm^{-1}, which is ascribed to δas NH_3, also decreased and finally disappeared after evacuation at 400 °C. These results suggest that the NH_3 decomposed completely at high temperatures over the Mn/TiO_2 catalyst. It is evident that a small amount of ammonia converted into N_2O and NO due to the

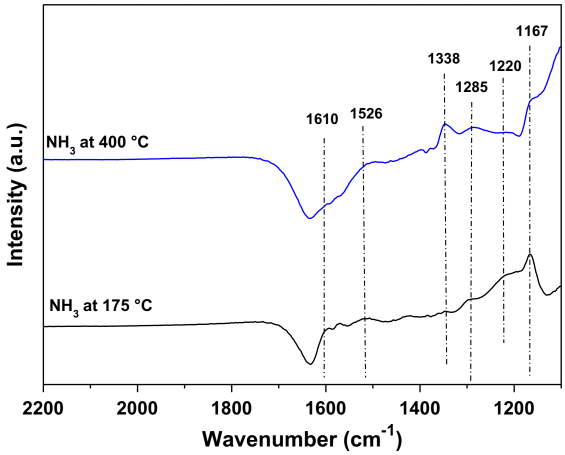

Fig. 6. *In situ* FT-IR spectra of coordinatively held ammonia species, adsorbed at 50 °C over the Mn/TiO_2 catalyst and evacuating at 175 and 400 °C.

ammonia oxidation at below 200 °C. Increase in the SCR reaction temperature monotonically enhanced the ammonia oxidation. These *in situ* FT-IR results are in very good agreement with our transient isotopic labeling studies.

3.2.7. Investigation of the evolution of NH_3 + NO reaction

It was interesting to investigate whether the catalyst is capable to perform the SCR reaction without the addition of oxygen or not. For this purpose, only ammonia and nitric oxide were fed through the catalyst bed. The signals for the mass numbers of NH_3 ($m/e = 16$), NO ($m/e = 30$), N_2 ($m/e = 28$), H_2O ($m/e = 18$), and N_2O ($m/e = 44$) were observed, when the ammonia and nitric oxide were introduced to the system. The reaction was observed for 3 h. Since no labeled gas was used for this experiment, only one species for each gas could be observed. Hence, the normalized concentrations of the species were gained by dividing the partial pressure of each species at a certain time by the partial pressure of the species at the end of the experiment (after 3 h). The Fig. 7 shows only the period of the first 80 min of reaction, since no change in the transient signal of the species was observed after 80 min of the reaction. It was found that after a short startup period of about 2–3 min, the SCR reaction took place. This is indicated by a drop of the concentrations of NO and NH_3 while the signals for nitrogen, nitrous oxide, and water increased (Eqs. (8) and (9)).

$$2NH_3 + 8NO \rightarrow 5N_2O + 3H_2O \tag{8}$$

$$4NH_3 + 6NO \rightarrow 5N_2 + 6H_2O \tag{9}$$

It is worth noting that the signal of ammonia was longer than that for NO. This is due to the ammonia oxidation which started simultaneously with the SCR reaction and prevented the high increase of the ammonia signal. The sharp increase of the nitrogen signal at the beginning is attributed to the sudden introduction of ammonia and nitric oxide, which also contain nitrogen. The SCR reaction could be observed for about 15 min before the NO concentration and the ammonia concentration increased again while the signals for nitrogen and water concentration steadily decreased. The signals of water and nitrous oxide did not decrease as fast as the nitrogen signal. The study thus indicated that the rate of SCR reaction is very small in the absence of gas phase oxygen and enhanced distinctly by the addition of excess oxygen. This implies that the contribution (supply) of oxygen with the nitric oxide is too small to fill up oxygen vacancies on the catalyst arising from the ammonia oxidation and the

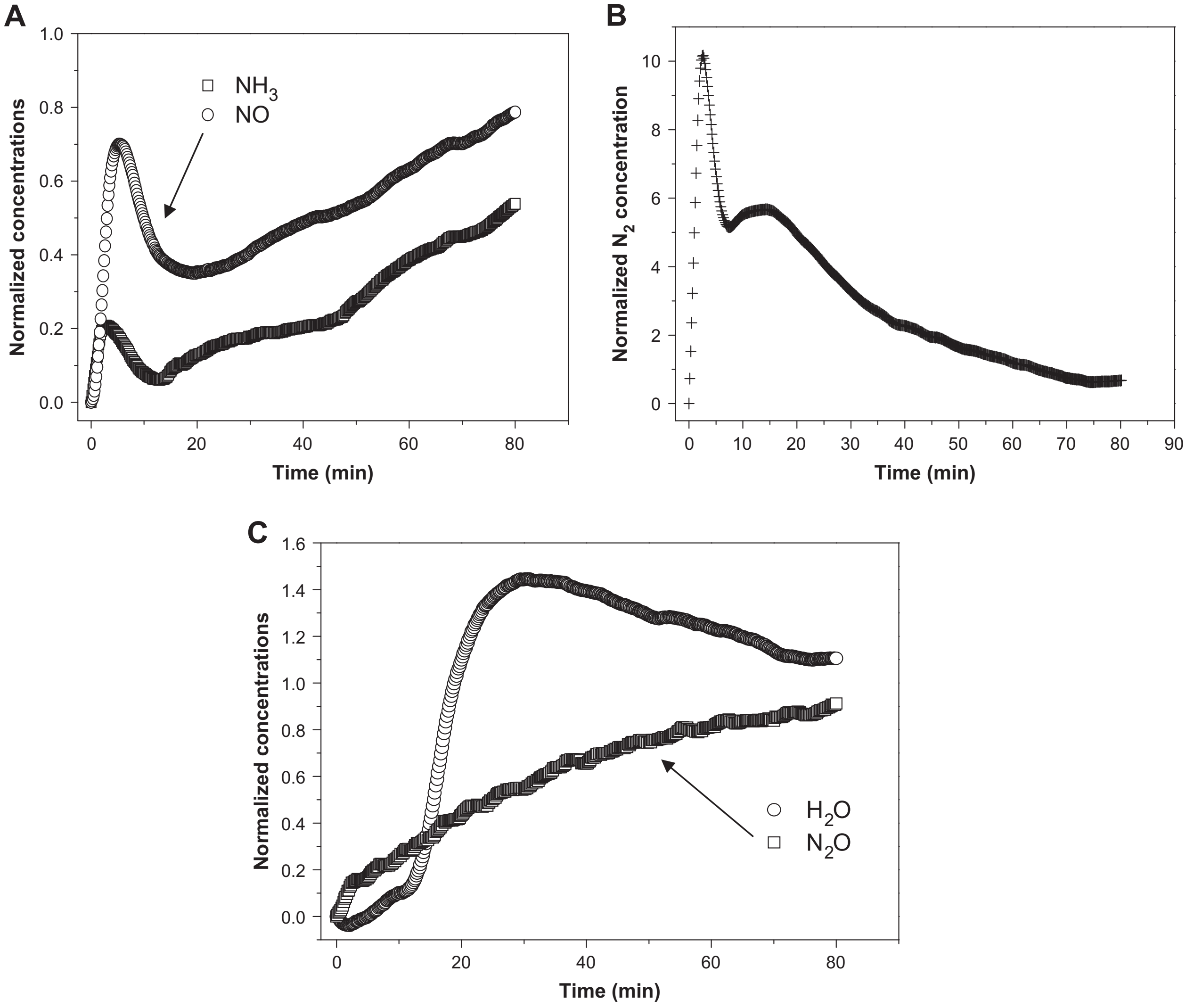

Fig. 7. Transient curves of the normalized concentrations of (A) ammonia and nitric oxide, (B) nitrogen, (C) water and nitrous oxide.

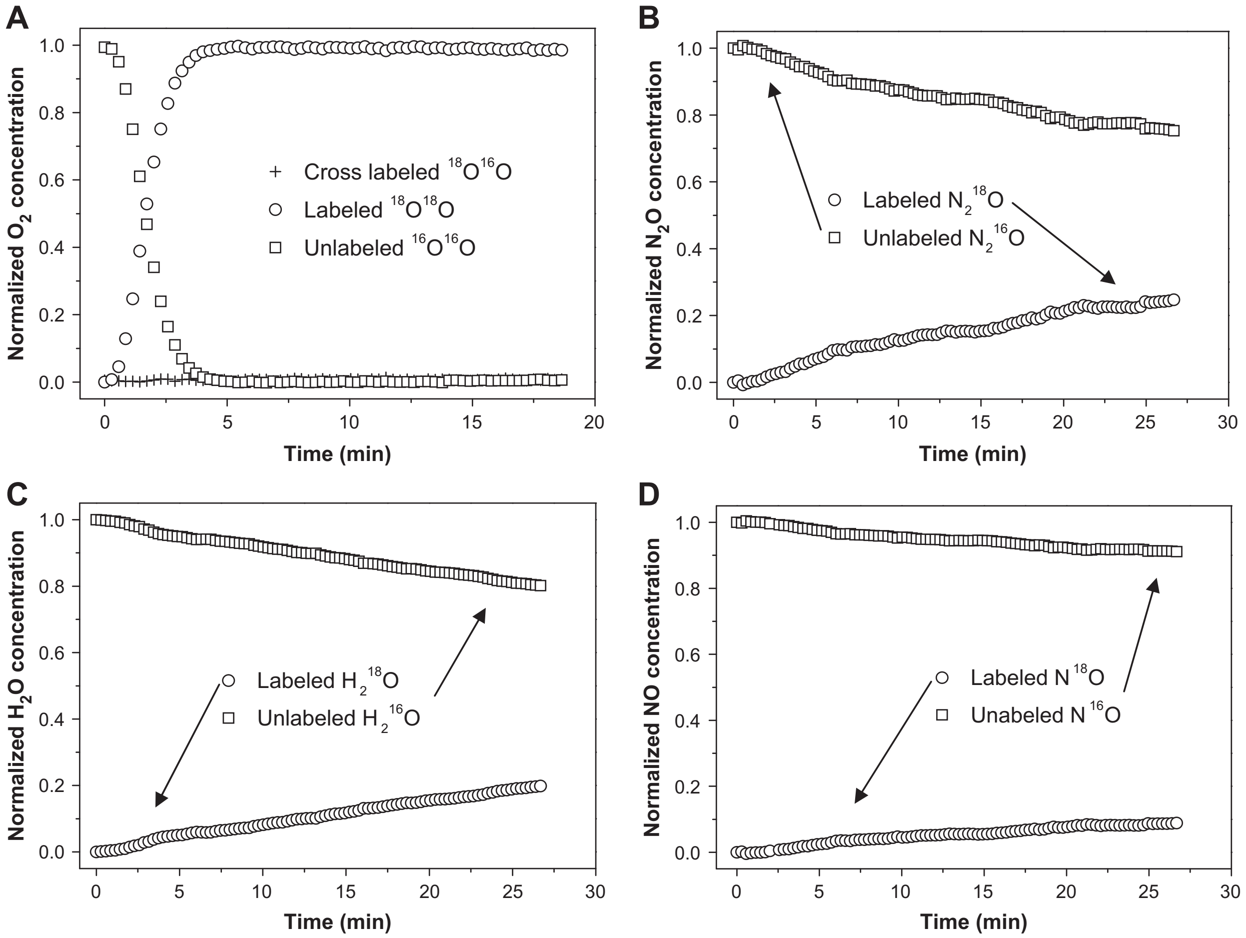

Fig. 8. Normalized concentrations of (A) oxygen, (B) nitrous oxide, (C) water, and (D) nitric oxide depending on the time in the SCR oxygen labeling experiment.

SCR reaction. This agrees with the literature where it was reported that excess oxygen is necessary to run the SCR reaction [32,33].

3.2.8. Investigation of the SCR reaction with O_2 labeling ($NH_3 + NO + {}^{16}O_2$) switched to ($NH_3 + NO + {}^{18}O_2$)

The first SCR experiment was done with labeled oxygen (${}^{18}O_2$). As in the ammonia oxidation study presented earlier, the similar signals for oxygen containing products (water, nitric oxide, oxygen, and nitrous oxide) were observed. The results are presented in Fig. 8. The interference of labeled nitric oxide ($N^{18}O$) with the unlabeled oxygen (${}^{16}O_2$) was too big to derive any conclusions for the transient state (due to the equal amu). However, it was possible to collect data for the nitric oxide at the pseudo steady state after the oxygen labeling (Table 1). It can be seen that the shapes of the transient curves are similar to those from the ammonia oxidation study. However, in contrast to this, the curves for nitric oxide and nitrous oxide reach a pseudo steady state. This is in agreement with the observations from the SCR experiment with ammonia labeling. The pseudosteady state values for the fractions of the $N^{18}O$ and $N_2{}^{18}O$ are close to the values of species representing the products of the ammonia oxidation in the ammonia labeling SCR experiment. The $N^{18}O$ and the $N_2{}^{18}O$ must be due to the oxidation of ammonia as only by this way the labeled oxygen can be incorporated in these products in such a high quantities. The oxygen exchange with the catalyst surface, where labeled oxygen is incorporated in the catalyst surface, does not provide enough $N^{18}O$ to explain the large amounts of $N_2{}^{18}O$ and $N^{18}O$ detected in this experiment. A further hint for this is the pseudosteady state for the $N^{18}O$ and the $N_2{}^{18}O$ after the labeling, because only a certain fraction of ammonia seems to be oxidized. An interesting observation is that water is likely to be formed by the same mechanism as in the ammonia oxidation since no significant difference in the shape of the transient curve for water could be observed. The concentration of cross-labeled oxygen is close to zero which supports the claim that the lattice oxygen is not labile in the presence of gas phase oxygen.

3.2.9. Investigation of the SCR reaction with NH_3 labeling (${}^{14}NH_3 + NO + O_2$ switched to ${}^{15}NH_3 + NO + O_2$)

The second study of the SCR reaction included the labeling of ammonia. In general, it can be said that the results of ammonia labeling reproduce the data from the previous experiments very well. The most important difference in comparison with the labeled oxygen experiment is the very long residence time of the ammonia in the system; because the replacement of the unlabeled ammonia from the system was not completed even after 40 min.

The long residence time of the ammonia implies that the surface residence time on the catalyst is longer than other gases such as nitric oxide. In this study, the cross-labeled nitrogen species arose from the reaction, which contains one nitrogen atom from labeled ammonia and another from unlabeled nitric oxide (Eqs. (10)–(12)).

$$2Mn^{4+} + 2{}^{15}NH_3 \rightarrow 2Mn^{3+} + 2{}^{15}NH_2 + 2H^+ \tag{10}$$

$$2Mn^{3+} + 2H^+ + 1/2O_2 \rightarrow 2Mn^{4+} + H_2O \tag{11}$$

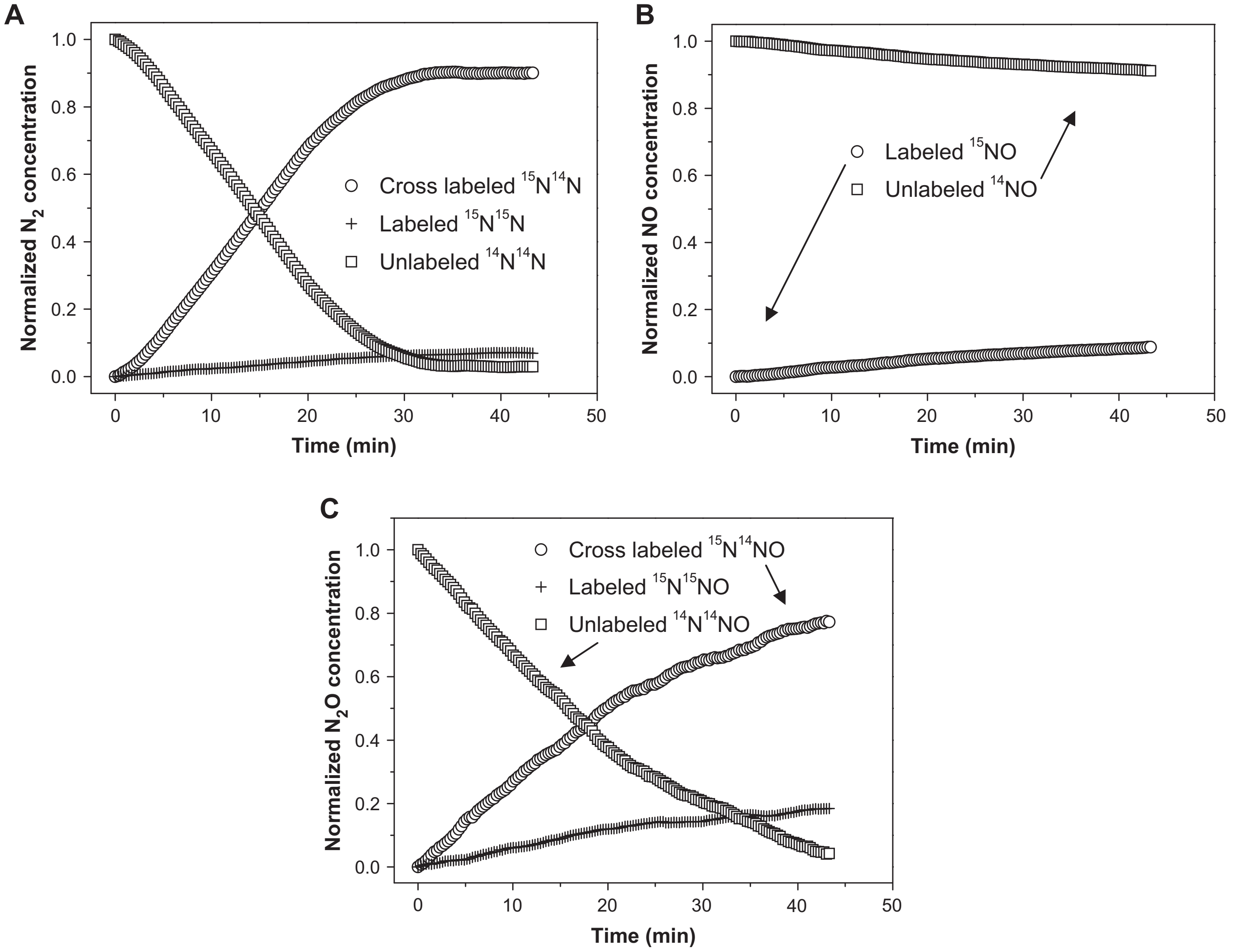

Fig. 9. Normalized concentration of (A) nitrogen, (B) nitric oxide, and (C) nitrous oxide versus time in the SCR ammonia labeling experiment.

$$2^{15}NH_2 + 2^{14}NO \rightarrow 2^{15}NH_2\text{-}^{14}NO \rightarrow 2^{15}N - {}^{14}N + 2H_2O \qquad (12)$$

Labeled species, where only ^{15}N atoms are incorporated, are due to ammonia oxidation [25]. Usually, in the pseudosteady state after the switching of labeled gas, the concentration of unlabeled nitrogen and nitrous oxide must be zero when the results from the NO reduction experiment are considered. The long residence time of the ammonia in the system could be explained due to the strong adsorption of ammonia on the catalyst surface. Although the catalyst can easily oxidize ammonia [29], it was found from the *in situ* FT-IR studies that there are ammonia species which are not oxidized rapidly and remain over the surface of catalyst even at higher temperatures for a long time. From the results presented in Fig. 9, one can observe that the largest fractions of nitrogen and nitrous oxide are obtained due to the coupling reaction between labeled ammonia and unlabeled nitric oxide in the SCR reaction. Thus, all the nitrous oxide made from a combination of $^{15}NH_3$ and ^{14}NO retains the starting nitrogen–oxygen bond. It is remarkable to note that the fraction of nitrous oxide arising from the ammonia oxidation is larger than that of nitrogen. The origin of unlabeled species was already discussed. The nitric oxide before the labeling is composed of unreacted nitric oxide and the formation of nitric oxide is due to the ammonia oxidation. The labeled nitric oxide after the switch to $^{15}NH_3$ indicates that the amount of ^{15}NO is due to ammonia oxidation, rather than the exchange $^{15}NH_3$ and ^{14}NO, since no concurrent formation of ^{15}NO was detected. The results from the ammonia and oxygen labeling of the SCR reaction are summarized in Table 2.

3.2.10. Investigation of the SCR reaction with NO labeling ($NH_3 + {}^{14}NO + O_2$ switched to $NH_3 + {}^{15}NO + O_2$)

The final study was the SCR reaction with labeled NO. The results of this study can be used to validate the data from the ammo-

Table 2
Values for the normalized concentration of different species gained labeling ammonia and oxygen in the SCR reaction.

	$^{15}NH_3$ labeling	$^{18}O_2$ labeling
Nitrogen due to ammonia oxidation	0.069 (unsteady state)	
Nitrogen due to SCR reaction	0.901 (unsteady state)	
Nitric oxide due to ammonia oxidation	0.088 (unsteady state)	0.088
Unreacted nitric oxide	0.912 (unsteady state)	0.912
Nitrous oxide due to ammonia oxidation	0.185 (unsteady state)	0.246
Nitrous oxide due to coupling between NH_3 and NO	0.772 (unsteady state)	0.754

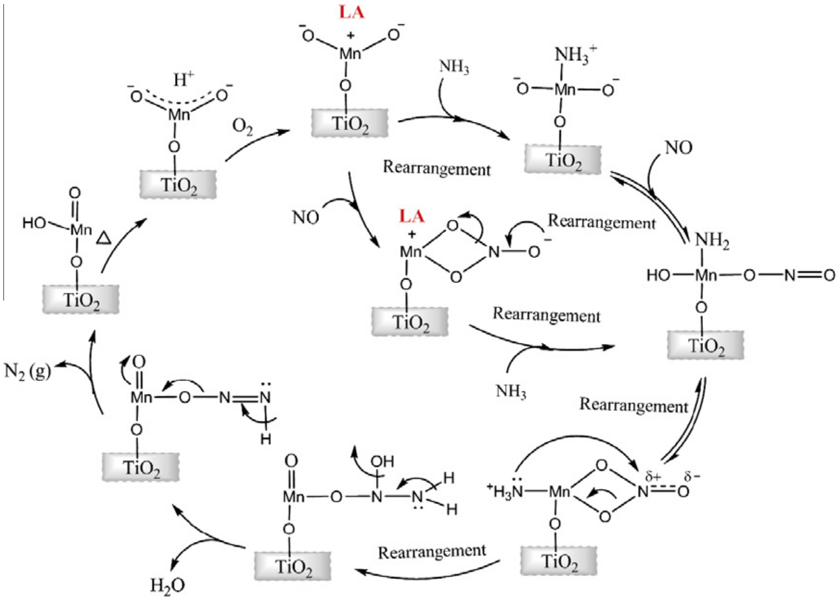

Scheme 1. Plausible SCR mechanism over the surface of titania-supported manganese catalysts.

nia labeling. Similar to the ammonia labeling, all cross-labeled species arose from the coupling of one nitrogen atom from the ammonia (^{14}N) and one from nitric oxide (^{15}N) in the SCR reaction. Unlabeled nitrogen, unlabeled nitric oxide, and unlabeled nitrous oxide are due to the ammonia oxidation reaction. Therefore, for the titania-supported manganese catalyst in the presence of oxygen, nitrous oxide is derived from the combination of two reactants ($^{14}NH_3 + {}^{15}NO$). The increasing amount of ammonia oxidation at the reaction temperature (i.e., 175 °C) preferentially forms nitrogen, not nitrous oxide (Eq. (13)).

$$2^{15}NO + 2NH_3 + 1/2O_2 \rightarrow 2^{14}N - {}^{15}N + 3H_2O \qquad (13)$$

4. Conclusions

In the present study, it has been found that the gas phase oxygen which makes oxidation–reduction process with respect to labile oxygen species on the catalyst surface, which is extremely important for the low-temperature SCR of NO_x with NH_3 over MnO_x/TiO_2 catalysts. The lattice oxygen is involved in the ammonia oxidation reactions and the SCR reaction is not able to take place without excess oxygen. Although the direct participation of excess oxygen is less in the reaction, it is highly significant for the filling of oxygen vacancies over the catalyst surface by the gas phase oxygen. It was found that the gas phase oxygen can exchange with the lattice oxygen, even if this happens only in small amounts. Furthermore, it was shown that nitric oxide is capable of exchanging oxygen with the catalyst, when it adsorbs on the catalyst surface. This complies with the results of the *in situ* FT-IR studies we performed, where it was found that NO can adsorb over the catalyst surface also at temperatures higher than 323 K. An interesting result is that the very long surface residence time of ammonia over the surface of catalyst. Furthermore, it was shown that the products and active intermediates of the SCR reaction are mainly due to a coupling of one nitrogen atom from ammonia and other one from nitric oxide. This result is in line with literature reports that obtained for other catalyst systems [14]. Furthermore, the sharp decrease of the unlabeled species $^{16}O^{16}O$ response (Fig. 5B open tetra angle) on NH_3 introduction (at t = fraction of minute in Fig. 5B) is evident of the instantaneous reaction of surface oxygen species with ammonia. It was found that the water is not formed directly with the gas phase oxygen. As it was proved that the oxygen from the lattice is participating in the SCR reaction by filling oxygen gaps, the reaction is more likely a Mars–van-Krevelen-like mechanism. Initially, the oxygen molecule from the catalyst surface reacts before it is replaced by gas phase oxygen. In connection with the results of FT-IR studies, in which the potential intermediate species were identified [21], and under consideration of the role of the oxygen, the following mechanism for the low-temperature SCR of NO_x over titania-supported manganese catalysts is proposed (Scheme 1).

Acknowledgment

The authors wish to acknowledge financial support from the National Science Foundation (Grant No. NSF-0828226).

References

[1] T. Ishihara, M. Ando, K. Sada, K. Takiishi, K. Yamada, H. Nishiguchi, Y. Takita, J. Catal. 220 (2003) 104–114.
[2] A.K.H. Nohman, D. Duprez, C. Kappenstein, S.A.A. Mansour, M.I. Zaki, in: B. Delmon, P.A. Jacobs, G. Poncelet (Eds.), Preparation of Catalysts V, Elsevier, Amsterdam, 1991, p. 617.
[3] C. Lahousse, A. Bernier, P. Grange, B. Delmon, P. Papaefthimiou, T. Ioannides, X. Verykiosy, J. Catal. 178 (1998) 214.
[4] C. Reed, Y. Xi, S.T. Oyama, J. Catal. 235 (2005) 378.
[5] P.G. Smirniotis, D.A. Pena, B.S. Uphade, Angew. Chem. Int. Ed. Engl. 40 (2001) 2479.
[6] B. Thirupathi, P.G. Smirniotis, J. Catal. 288 (2012) 74–83.
[7] B. Thirupathi, P.G. Smirniotis, Appl. Catal. B: Environ. 110 (2011) 195–206.
[8] D.A. Pena, B.S. Uphade, P.G. Smirniotis, J. Catal. 221 (2003) 421.
[9] P.R. Ettireddy, N. Ettireddy, S. Mamedov, P. Boolchand, P.G. Smirniotis, Appl. Catal. B: Environ. 76 (2007) 123.
[10] J.H.B.J. Hoebink, J.P. Huinink, G.B. Marin, Appl. Catal. A: Gen. 160 (1997) 139.
[11] A.M. Efstathiou, X.E. Verykios, Appl. Catal. A: Gen. 151 (1997) 109.
[12] Q. Sun, Z.-X. Gao, H.-Y. Chen, W.M.H. Sachtler, J. Catal. 201 (2001) 89–99.
[13] U.S. Ozkan, C. Yeping, M.W. Kumthekar, J. Catal. 149 (1994) 375.
[14] U.S. Ozkan, C. Yeping, M.W. Kumthekar, J. Catal. 149 (1994) 390.
[15] J.P. Breen, R. Burch, C. Hardacre, C.J. Hill, C. Rioche, J. Catal. 246 (2007) 1–9.
[16] B.L. Duffy, H.E.C. Hyde, N.W. Cant, P.F. Nelson, J. Catal. 149 (1994) 11–22.
[17] Y.Z. Steenwinkel, L.M. van der Zande, H.L. Castricum, A. Bliek, App. Catal. B: Environ. 54 (2004) 226–236.
[18] M.R. Smith, U.S. Ozkan, J. Catal. 142 (1993) 226–236.
[19] B. Thirupathi, P.G. Smirniotis, Catal. Lett. 141 (2011) 1399–1404.
[20] D.A. Pena, B.S. Uphade, E.P. Reddy, P.G. Smirniotis, J. Phys. Chem. B 108 (2004) 9927.
[21] F.E. Massoth, Adv. Catal. 27 (1978) 265.
[22] F. Kapteijn, J. Dick van Langeveld, J.A. Moulijn, A. Andreini, M.A. Vuurman, A.M. Turek, J.-M. Jehng, I.E. Wachs, J. Catal. 150 (1994) 94.

[23] G. Basca, L. Lietti, G. Ramis, F. Berti, Appl. Catal. B: Environ. 18 (1998) 1.

[24] G. Busca, V. Lorenzelli, J. Catal. 72 (1981) 303.

[25] K. Margarita, J. Catal. 204 (2001) 479–494.

[26] K. Hadjiivanov, V. Bushev, M. Kantcheva, D. Klissurski, Langmiur 10 (1994) 464.

[27] K. Nakamoto, Infrared and Raman Spectra of Inorganic and Coordination Compounds, fourth ed., Wiley, New York, 1986.

[28] F. Kapteijn, L. Singoredjo, M. van Driel, A. Andreini, A.M. Jacob, G. Ramis, G. Busca, J. Catal. 150 (1994) 105–116.

[29] J.M.G. Amores, V.S. Escribano, G. Ramis, G. Busca, Appl. Catal. B: Environ. 13 (1997) 45.

[30] G. Qi, R.T. Yang, Appl. Catal. B: Environ. 44 (2003) 217.

[31] J. Pérez-Ramírez, E.V. Kondratenko, J. Catal. 250 (2007) 240–246.

[32] M. Inomata, A. Miyamoto, T. Ui, K. Kobayashi, Y. Murakami, Ind. Eng. Chem. Prod. Res. Dev. 21 (1982) 424.

[33] B.L. Duffy, H.E.C. Hyde, N.W. Cant, P.F. Nelson, J. Phys. Chem. 97 (1993) 1729–1732.